Effect of microchannel wall dimensions and temperature on ethylene glycol fluid's thermal performance in two-dimensional microchannels using molecular dynamics simulation

Linxiang Li [1], Hadi Bagheri [2], S. Mohammad Sajadi [3], Chunsheng Yang [4], Darius Andriukaitis [5], Z. Li [6], Xiaofei Wen [7,*], Mustafa Inc [8,9]

[1] School of Engineering, Ocean University of China, Qingdao 266001, China
[2] Department of Mechanical Engineering, Najafabad Branch, Islamic Azad University, Najafabad, Iran
[3] Department of Nutrition, Cihan University-Erbil, Kurdistan Region, Iraq
[4] National Research Council Canada, Aerospace Research Centre, Ottawa K1A 0R6, Canada
[5] Department of Electronics Engineering, Kaunas University of Technology, Kaunas 51368, Lithuania
[6] Faculty of Mechanical Engineering, Opole University of Technology, Opole 45758, Poland
[7] Donghai Laboratory, Zhoushan 316021, China
[8] Science Faculty, Department of Mathematics, Firat University, Elazig 23119, Turkey
[9] Department of Medical Research, China Medical University, Taichung 40402, Taiwan

ARTICLEINFO

Keywords:
Engine cooling
Thermal behavior
Ethylene glycol
MC
Molecular dynamics simulation

ABSTRACT

Increasing the transfer (HT) coefficient used in thermal industries is very important. Various methods are used to improve the efficiency of thermal heat HT so that maximum HT takes place in a smaller space. Ethylene glycol (EG) is generally used as an agent for convective HT. EG obtains energy from a hot source and discharges it to the required location. At present, the most consumption of EG is to produce engine cooling fluid. In the upcoming research, the TB of EG fluid in two-dimensional microchannels(MCs) has been investigated using molecular dynamics (MD) simulations, and the effect of variables such as MC dimensions and MC wall temperature(Temp) on the TB of the simulated fluid has been investigated. The results revealed that by increasing the Temp dif- ference of the MC wall from 10 to 50 K, the maximum temperature (Max-Temp) and velocity (Max-Vel) of the target sample increased to 640.94 K and 0.024 Å/ps. It can be concluded that the increase in the cross-sectional area and the wall Temp difference leads to an increase in the HT rate in the MC.

1. Introduction

Nowadays, the problem of improving HT in engineering sciences and various industrial applications has been increasing. It has attracted the attention of many researchers, so it has become an essential part of experimental and theoretical research [1–3]. Increasing the HT coefficient used in thermal industries is very important. Various methods are used to increase thermal HT efficiency so that maximum HT takes place in a smaller space. Improving HT using conventional methods has significantly saved energy costs and resources and preserved the environment [4–6]. The convection method mainly uses EG as an agent for HT. EG is usually used in air conditioning, cold water systems, or cars with liquid cooling fluid. At present, the most consumption of EG is to produce engine cooling fluid. EG is used as an antifreeze in cars and machines. In the cooling system of cars, EG liquid plays the basic function of dealing with freezing. But due to the corrosiveness of this substance, anti-corrosion inhibitors are added to it to prevent rusting [7–10].

Many papers have been done on TB and improving the thermal performance of various fluids, and some have been briefly discussed. For instance, Guo et al. [11] investigated external heat's effect on the base fluid's TB in an MC. In this study, EG was considered as the base fluid.

The obtained results revealed that an increase in Temp leads to an increase in entropy and subsequently the improvement of HT in the studied fluid. Bagheri et al. [12] investigated the forced convection HT in a thermal MC with H_2O /alumina and H_2O /copper oxide NFs. They discussed the effect of hydraulic diameter and volume fraction of NPs on HT. This study revealed that increasing the volume fraction of NPs and decreasing the diameter of NPs increases the value of the Nusselt number. Wu et al. [13] examined the effect of nanochannel roughness on the thermal performance of fluid in a nanochannel. The results revealed that increasing the nanochannel roughness can disturb the TB of the fluid. Kalteh et al. [14] investigated the effect of Nps' volume

* Corresponding author.
E-mail address: wenxiaofei@zjou.edu.cn (X. Wen).

Table 1
The parameters of 1. LJ potential functions [27,28].

Particle type	σ (Å)	ϵ (kcal/mol)
H	2.886	0.044
O	3.500	0.06
C	3.851	0.105
Pt	2.754	0.080

percentage and diameter on the TB of the studied NF in an MC. The obtained results revealed that the TB of NF improves by increasing the volume fraction of NPs and decreasing the diameter of NPs. Rostami et al. [15] investigated the effect of cubic roughness on the TB of argon fluid inside a platinum MC. Hu et al. [16] examined the effect of MC type on the atomic AB of fluid in an MC. The results revealed that changing the channel type can increase the atomic stability of the whole system. Shang et al. [17] examined the MC thickness on the AB of NF. The results revealed that with the increase of wall thickness, the atomic displacement decreases and the results indicate the aggregation process in the structure. Chen and Ding [18] analyzed an MC heat sink's HT characteristics and cooling performance with H_2O / alumina NFs with different volume fractions of NPs.

Previous studies revealed that the effect of channel wall Temp, dimensions, and cross-sectional area on the atomic and thermal performance of EG in a two-dimensional MC has not been investigated. Therefore, the TB of the desired fluid in the two-dimensional MC has been investigated in the current study. By studying and reviewing the research done so far, it can be seen that few studies have been done in determining the thermal properties of EG fluid in a two-dimensional platinum MC using the MD simulation [16–19]. Therefore, in this research, the effects of MC wall Temp difference and MC dimensions and cross-sectional area on physical parameters such as density, Temp, velocity, and thermal parameters such as HF and TC have been evaluated using LAMMPS software and MD simulation.

2. Simulation method

2.1. The MD method

Nowadays, MD is widely used in various engineering and basic sciences. Analytical determination of complex molecular systems' characteristics is impossible due to a large number of particles [19,20]. Therefore, it can be solved using the calculation method defined in the MD simulation. Newton's equations of motion are fundamental relationships in the MD. Solving these equations for each particle of the system leads to determining the movement path of all particles over time [21,22]:

$$F_i = m_i a_i = -\nabla_i U = -\frac{dU}{dr_i} \tag{1}$$

In relation (1), m_i represents the mass of the i particle, and in the relations discussed, the acceleration is also obtained according to relation (2) [21,22]:

$$a_i = \frac{d^2 r_i}{dt^2} \tag{2}$$

In relation (2), r_i is a vector that specifies the position of the particle. From the combination of the above relations, relation (3) is obtained [21,22]:

$$-\frac{dU}{dr_i} = m_i \frac{d^2 r_i}{dt^2} \tag{3}$$

One of the standard numerical integration methods is the velocity-relations (4) and (5) [23,24]:

$$r_i(t+\Delta t) = r_i(t) + \left(\frac{dr_i}{dt}\right)\Delta t + \frac{1}{2}\left(\frac{d^2 r_i}{dt^2}\right)(\Delta t)^2 + ... \tag{4}$$

$$r_i(t-\Delta t) = r_i(t) - \left(\frac{dr_i}{dt}\right)\Delta t + \frac{1}{2}\left(\frac{d^2 r_i}{dt^2}\right)(\Delta t)^2 + ... \tag{5}$$

The above relations, after simplification, can be expressed according to the following relation [23,24]:

$$r_i(t+\Delta t) = 2r_i(t) - r_i(t-\Delta t) + \left(\frac{d^2 r_i}{dt^2}\right)(\Delta t)^2 \tag{6}$$

$$v_i(t+\Delta t) = v_i(t) + \Delta t\, v_i(t) + \frac{\Delta t\,(a_i(t) + a_i(t+\Delta t))}{2} \tag{7}$$

TC coefficient (K) via Green-Kubo relation [25,26]:

$$K = \frac{V}{k_B T^2}\int_0^\infty J_x(0)\,J_x(t)\,dt = \frac{V}{3k_B T^2}\int_0^\infty J(0)\cdot J(t)\,dt \tag{8}$$

$$J = \frac{1}{V}\left[\sum_i e_i v_i - \sum_i S_i v_i\right]$$

$$= \frac{1}{V}\left[\sum_i e_i v_i - \sum_{i<j}\left(f_{ij} v_j\right) x_{ij}\right] \tag{9}$$

$$= \frac{1}{V}\left[\sum_i e_i v_i - \frac{1}{2}\sum_{i<j}\left(f_{ij}\cdot\left(v_i + v_j\right)\right) x_{ij}\right]$$

In the above equation, the parameters e_i and V respectively represent the total energy (for each particle) and the total volume of the sample. Also, in this equation, S_i represents the entropy of the system and v_i represents the velocity of the particle. Another factor that is very important in the MD method is the definition of the potential function to determine the force between the constituent particles of a structure [27].

Eq. (10) represents the potential function of Lennard Jones (LJ), which is used in the MD simulations to simulate interactions between different particles. This function has the potential of repulsion and attraction in its formulation [28].

$$U(r_{ij}) = 4\varepsilon\left[\left(\frac{\sigma}{r_{ij}}\right)^{12} - \left(\frac{\sigma}{r_{ij}}\right)^{6}\right] \quad \cdots r_{ij} \le r_c \tag{10}$$

The parameters of the LJ potential function are revealed in Table 1. Also, based on formulas (11) and (12), the values of σ and ϵ are obtained [28,29]:

$$\varepsilon_{ij} = \sqrt{\varepsilon_i \varepsilon_j} \tag{11}$$

$$\sigma_{ij} = \frac{\sigma_i + \sigma_j}{2} \tag{12}$$

In EAM, force-field atomic interaction is achieved as follows [30]:

$$U_i = F_\alpha\left(\sum_{j\neq i}\rho_\beta(r_{ij})\right) + \frac{1}{2}\sum_{j\neq i}\varphi_{\alpha\beta}(r_{ij}) \tag{13}$$

Verlet's algorithm [23,24]. This integration algorithm is according to

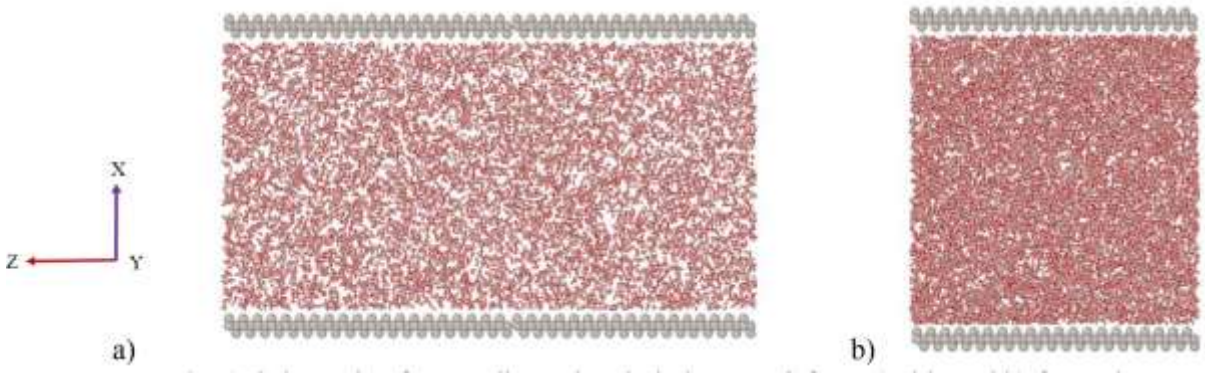

Fig. 1. Schematic of a two-dimensional platinum MC from (a) side and (b) front view.

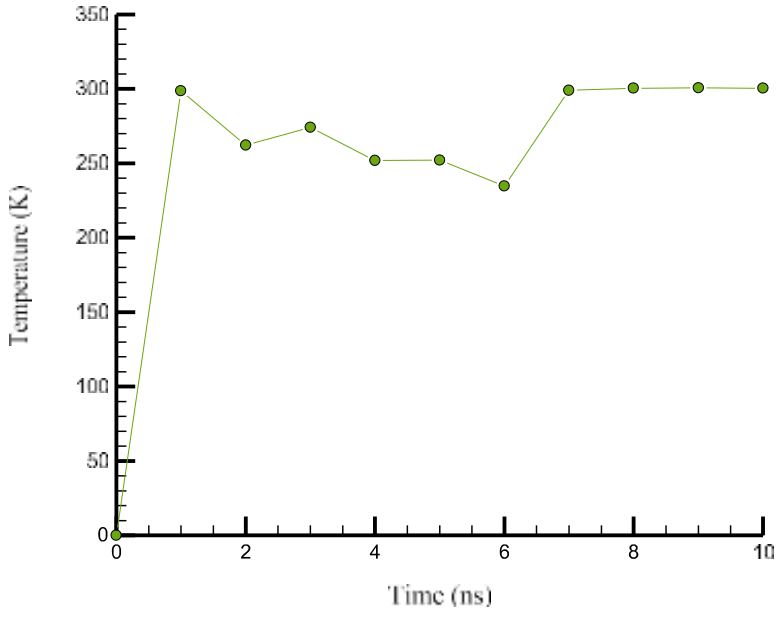

Fig. 2. Temp variations vs. the simulation time

1.1. Simulation details

This research used Avogadro and LAMMPS software to model the structure of EG and two-dimensional platinum MC. The dimensions of the SB in this study are $0.5_{\times} 0.5 \times 1\ \mu m^3$. The total number of present particles is 10,032 atoms. It is worth noting that the Z-degree boundary conditions are considered fixed, while these conditions are considered periodic in both the X and Y directions. In the first stages, it is necessary to make sure about the atomic modeling and the force field. In this step, the NVT ensemble (a constant volume and Temp ensemble) is used. The simulation time and time step used in these studies equals 20 ns and 1 fs. For this purpose, the desired fluid is balanced at the desired initial Temp (300 K). The initial Temp in the structures is balanced using the nose-Hoover thermostat. From the computational point of view, the balancing process in the current research was carried out for 10 ns. Fig. 1 demonstrates a schematic of the modeled structure. In the next step, the effect of MC wall dimensions and Temp on EG fluid's TB in the simulated MCs is examined. In this step, the NVE ensemble (a constant volume and energy ensemble) is used. These steps were examined during 10 ns.

reported. Fig. 2 reveals the Temp changes in the defined atomic sample to the simulation time. The results for this quantity indicate a decrease in

1.2. Stability process

The changes in thermodynamic quantities are investigated and

Temp fluctuations in this structure over time, indicating the appropriate settings applied in the current research. The Temp value in the whole atomic sample is equal to 300 K in the last time step. The Temp balance in the samples indicates the non-divergence of the oscillation amplitude of the structures within the SB, which indicates the stability of the structure. As a result, it can be said that the simulation time of 10 ns is sufficient in the balancing stage.

Also, the KE changes reveal similar behavior, and this quantity converges to the value of 17.35 eV after 10 ns. The changes in KE in the atomic sample with simulated time are presented in Fig. 3. Considering that the value of the second power of the velocity in the equation of KE is positive, as a result, this value is always positive. Convergence in KE with time results from decreasing mobility in atomic samples. By reducing the mobility of atoms inside the number of oscillations created decreases, and as a result, the structure reveals physical balance [31,32].

1.3. Validation

In the final part of this part, it will be useful to provide a correct quantity to validate the samples. For this purpose, the use of the simulated fluid radial distribution function (RDF) is presented in Fig. 4. The use of RDF indicates how the atoms in a structure are arranged relative to each other. In the analysis of the result obtained in this part, it can be said that there is a distinct peak and several times the liquid phase is revealed in the simulated base fluid sample, which somehow reveals the accuracy of the simulation method.

2. Results and discussion

As mentioned in the previous sections, the atomic and TB of EG fluid inside a two-dimensional platinum MC are investigated in the current research. For this purpose, in this section, the influence of factors such as the dimensions of the MC and the Temp difference of the walls on the atomic and TB of the fluid is reported. Also, in the present study, various physical quantities such as density, TC, velocity, and Temp and HF profiles have been calculated and reported.

2.1. Effect of wall Temp difference

After observing the simulated samples' thermodynamic equilibrium, the sample's atomic and TB are investigated. Creating a Temp difference in the MC walls can effectively move fluid atoms near the MC walls and,
finally, their atomic and TB. To investigate this issue, the Temp differ- ence between the two walls is considered equal to 10 K, 20 K, 30 K, and 50 K. The thermophysical parameters of density, Temp, velocity, HF, and TC have been calculated and reported. Fig. 5 reveals the atomic arrangement of EG fluid after applying a Temp difference of 10, 20, 30, and 50 K. According to Fig. 5, the simulated fluid is still stable by applying the Temp difference in the MC walls.

Fig. 6 reveals the maximum density (Max-Dens) changes in the simulated samples according to the Temp difference between the MC walls. According to Fig. 6, as the Temp difference in the sampleincreases, the maximum value of the density increases, and this increase occurs near the cold wall. As the wall Temp difference increases and due to the higher Temp near the hot wall, the density decreases. The exis- tence of HT from the hot wall to the fluid causes the KE of the fluid molecules to increase and the time of their presence in the force field of the wall to decrease significantly. As a result, the density in the vicinity of the hot wall decreases. As the Temp difference between the walls increases from 0 to 50 K, the Max-Dens value decreases from 0.025 $atom/Å^3$ to 0.3018 $atom/Å^3$.

Fig. 7 illustrates the Max-Temp changes in the simulated samples according to the Temp difference between the MC walls. By increasing the wall Temp difference, the effect of the wall Temp on the distribution of atoms near the wall increases. As a result, the process of HTs between the walls increases compared to the fluid atoms in the vicinity of the wall. As a result, the HTs between the wall and the fluid increase. As a result, by increasing the Temp difference between the walls from 0 to 50 K, the Max-Temp value increases from 514.35 K to 640.94 K.

Fig. 8. represents the Max-Vel changes in the simulated samples according to the Temp difference between the MC walls. According to the presented Fig. 8, with the increase of the Temp difference between the wall from 0 to 50 K, the Max-Vel value increases from 0.01 $Å/ps$ to 0.024 $Å/ps$. This increase is the result of increasing the HF applied to the particles, and as a result, their mobility and velocity increase. On the samples due to the increase in the Temp difference and the range of fluctuations. As a result, the Temp of the defined samples increases. This AB of samples should be considered in designing atomic structures for HT in industrial and confirmed applications.

After observing the atomic balance and stability and determining the structural evolution in the samples, changes in HF and TC are investigated according to the Temp difference. Fig. 9 reveals the HF of the simulated samples. Based on these results, it can be said that the increase in Temp difference causes an increase in the oscillation range and, as a result, an increase in the HF flowing inside the SB. The value of this quantity at the Temp difference of 10, 20, 30, and 50 K is equal to 1356, 1388, 1403, and 1459 W/m^2 after 10 ns.

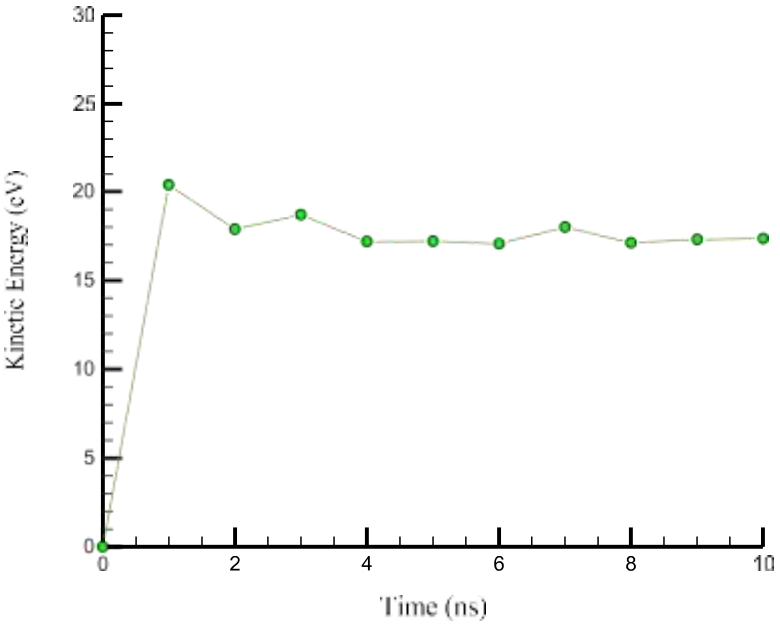

Fig. 3. KE variations vs. the simulation time.

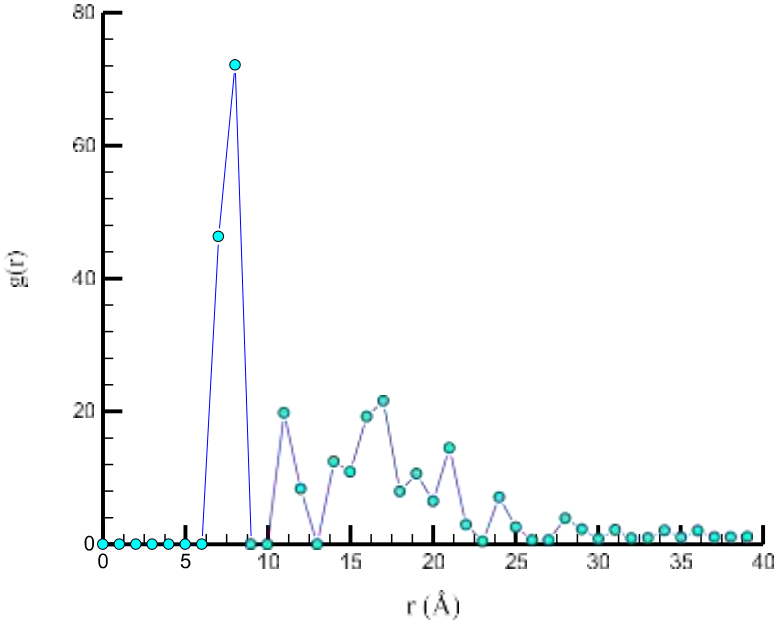

Fig. 4. The simulated fluid RDF.

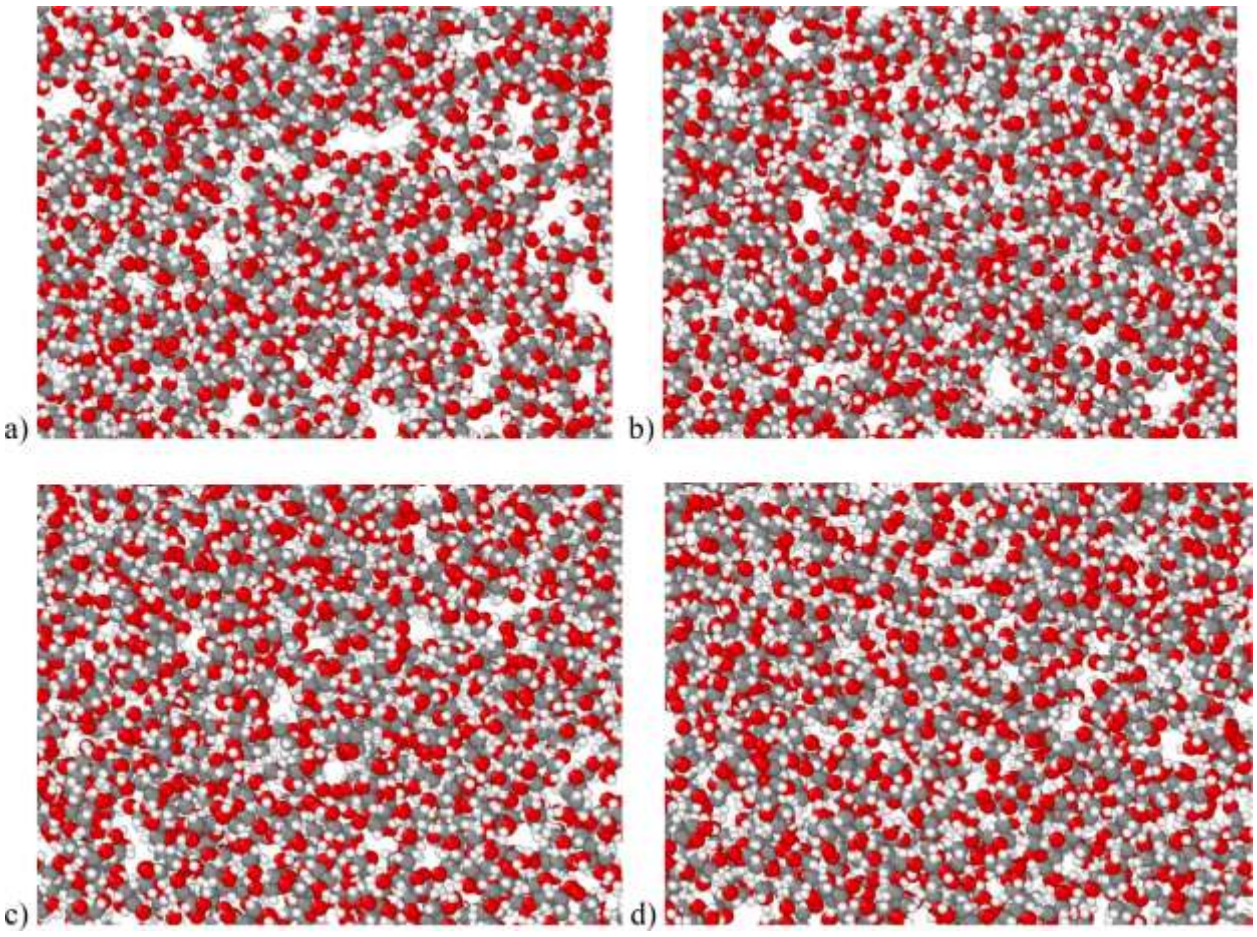

Fig. 5. The atomic arrangement of EG fluid after applying Temp difference with values of (a) 10, (b) 20, (c) 30, and (d) 50 K.

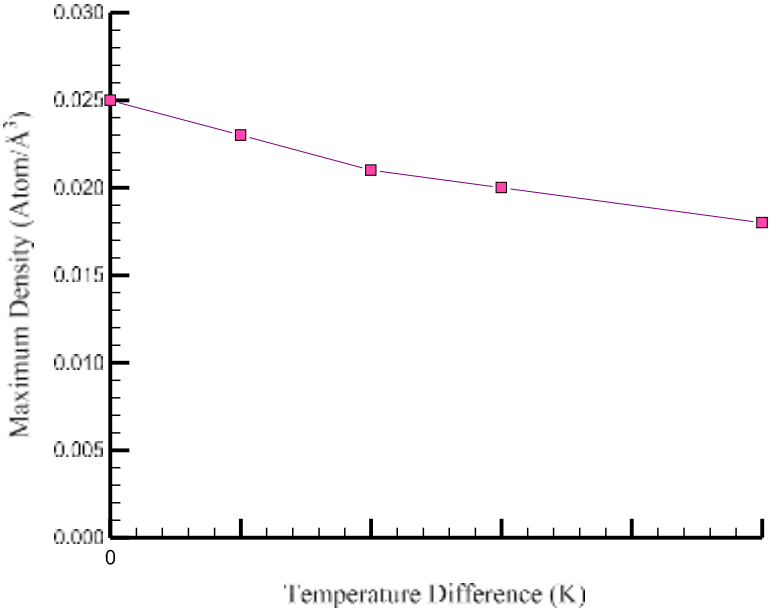

Fig. 6. Max-Dens variations in the simulated samples with the Temp difference.

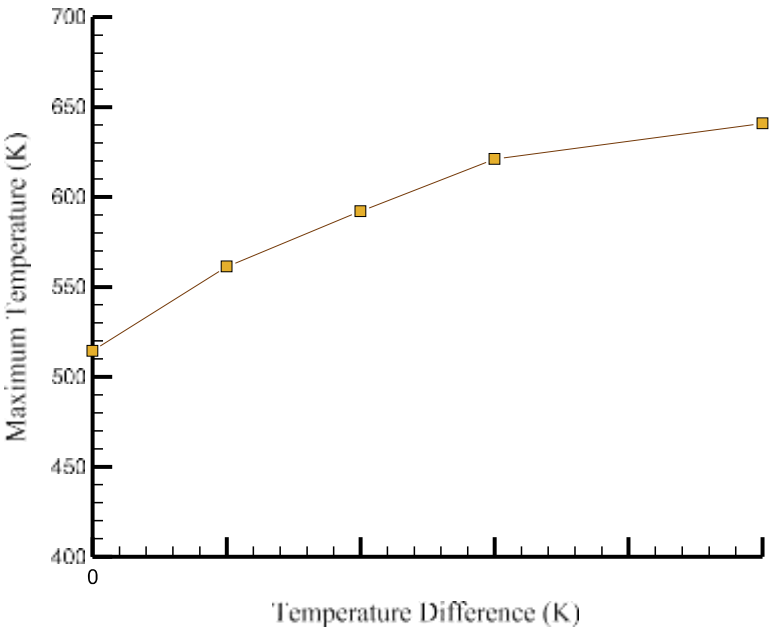

Fig. 7. Max-Temp variations with the Temp difference.

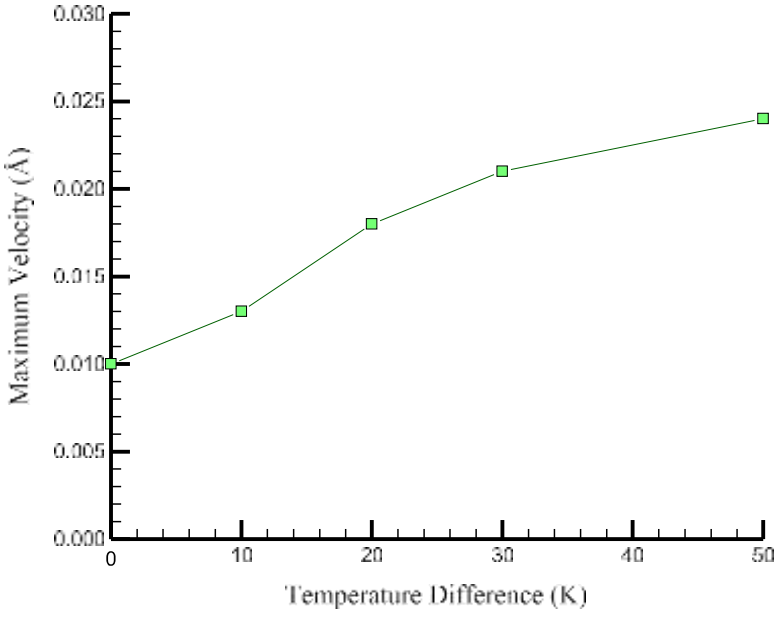

Fig. 8. Max-Vel variations with the Temp difference.

Fig. 10 in this section illustrates the TC of the simulated samples versus time in various Temp differences. By maximizing the HF by other hand, the stated process causes an increase in the movement of the

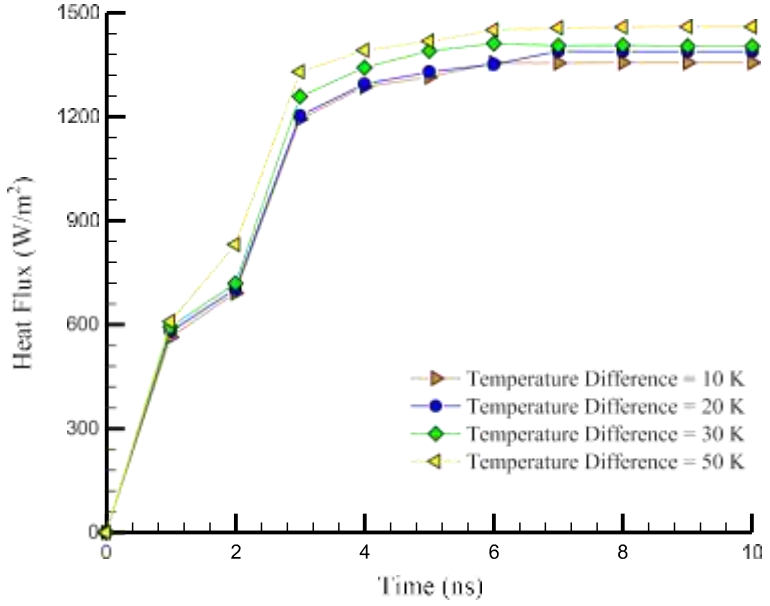

Fig. 9. Changes in the fluid's HF according to the MC wall's Temp difference.

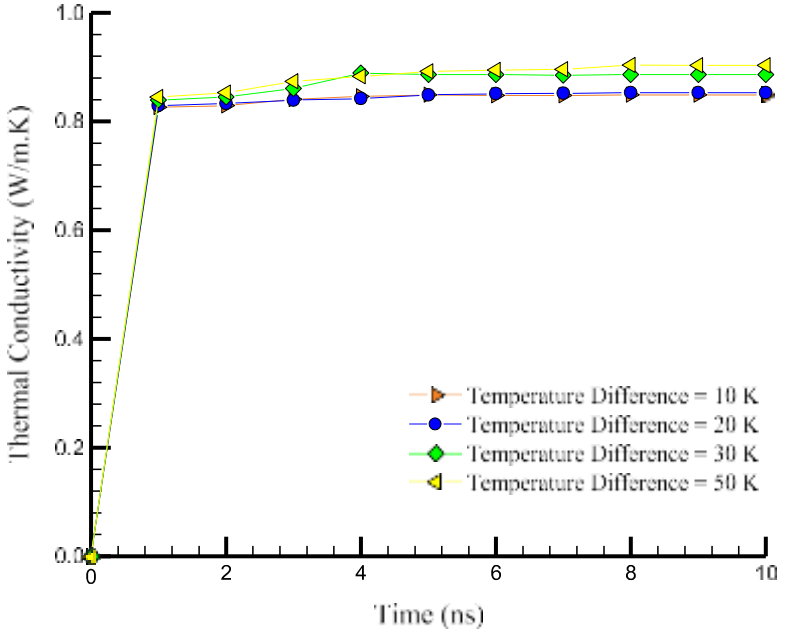

Fig. 10. Changes in the fluid's *TC* based on the MC wall's Temp difference.

Table 2

Numerical results of the simulated structure for the Temp difference of cold and hot walls.

Temp difference (K)	Max-Dens (atom/Å^3)	Max-Vel (Å/ps)	Max-Temp (K)	HF (W/m^2)	TC (W/m.K)
10	0.023	0.013	561.359	1356	0.849
20	0.021	0.018	592.011	1388	0.853
30	0.020	0.021	621.065	1403	0.886
50	0.018	0.024	640.943	1459	0.903

applying the Temp difference of the MC wall, the TC also increases so that the value of the TC at the Temp difference of 10, 20, 30, and 50 K after 10 ns, respectively, is equal to 0.849, 0.853, 0.886 and 0.903 W/m.K. As a result, the HT in industrial cases is expected to increase by increasing the Temp difference in the designed sample.

The numerical results obtained in this part of the research are presented in Table 2. Table 2 demonstrates the values of density, velocity, Temp, and thermal parameters (HF and TC) with increasing Temp differences of MC walls.

2.2. *The effect of MC dimensions*

The size of the cross-section of the defined MC is very influential in the fluid flow inside it. As a result, it can affect the simulated assembly's atomic transformation and thermal conduction. To investigate this issue, the platinum MC's cross-section size equals 0.25, 0.36, 0.49, and 0.56 Å^2. Fig. 11 represents the atomic arrangement of EG fluid in different MC cross-sections. According to the atomic structures presented in Fig. 11, the fluid sample has stability with the increase of the cross-sectional area

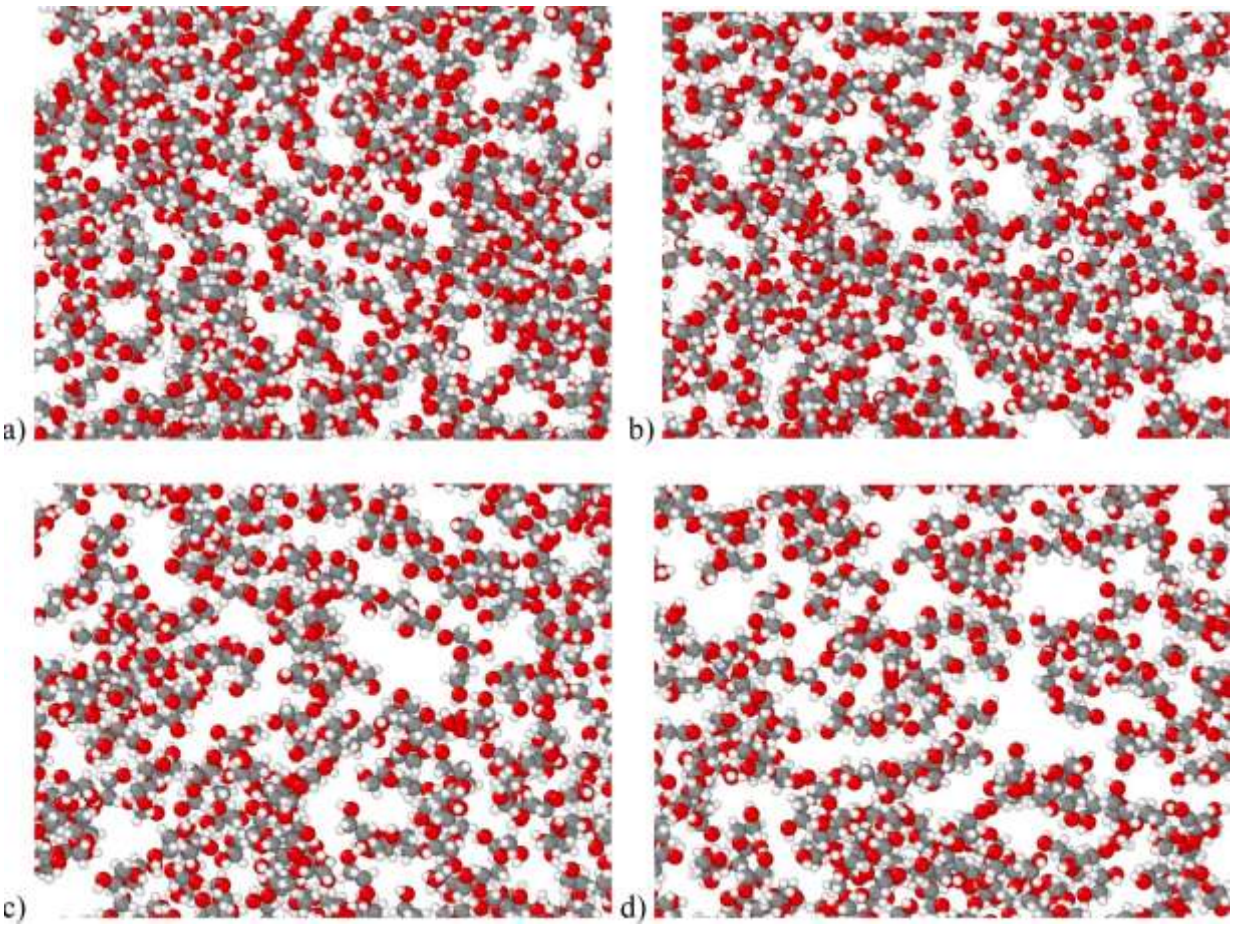

Fig. 11. The atomic arrangement of EG fluid according to the cross-sectional area of the MC (a) 0.25 Å^2, (b) 0.36 Å^2, (c) 0.49 Å^2, (d) 0.56 Å^2.

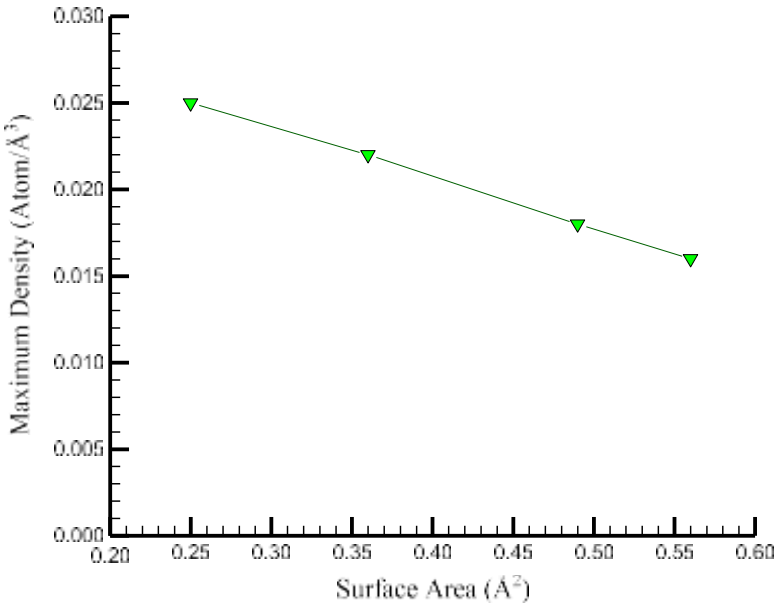

Fig. 12. Max-Dens changes according to MC cross-section.

of the MC.

Fig. 12 demonstrates the Max-Dens changes in the simulated samples according to the cross-sectional area of the MC. Based on the results obtained for the Max-Dens in the samples, it can be concluded that the Max-Dens decreases with the increase of the cross-sectional area. This behavior indicates that as the cross-sectional area of the MC increases, the flow intensity of EG decreases compared to the cross-sectional area at the Temp of 300 K. By increasing the cross-sectional area from 0.25 Å^2

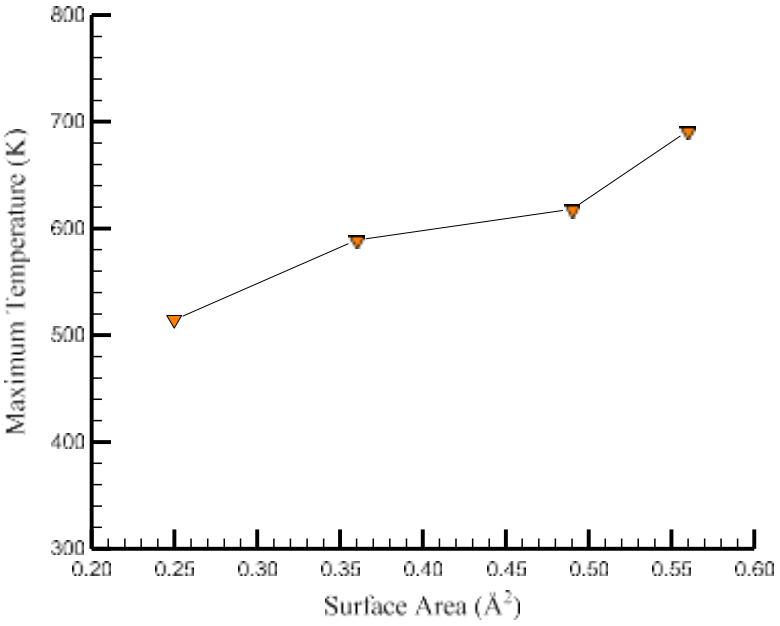

Fig. 13. Max-Temp changes according to MC cross-section.

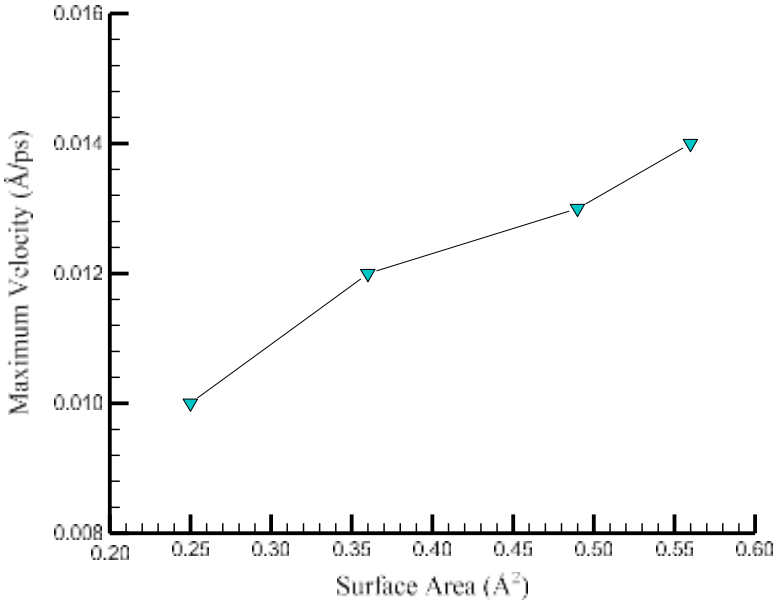

Fig. 14. Max-Vel changes according to MC cross-section.

to 0.56 $Å^2$, the Max-Dens value reaches from 0.025 $atom/Å^3$ to 0.016 $atom/Å^3$.

Increasing the cross-sectional area of the MC causes the absorbent force to enter the fluid particles with less intensity from the side of the walls. This increases the mobility of fluid particles, and as a result, the Max-Temp in the samples increases. Fig. 13 illustrates the Max-Temp changes in the simulated samples according to the cross-sectional area of the MC. According to the graph drawn in Fig. 13, with the increase of the cross-sectional area from 0.25 $Å^2$ to 0.56 $Å^2$, the Max-Temp value increases from 514.353 K to 691.639 K. This maximum value occurred in the middle regions of the MC, which had a greater distance from the walls. Because less force is applied to the fluid particles in this part from the side of the walls, they have the maximum movement and velocity. Therefore, the Temp has also reached the maximum value in this part.

Similar behavior can be seen for the Max-Vel in Fig. 14. Fig. 14 represents the Max-Vel changes in the simulated samples according to the cross-sectional area of the MC. By increasing the cross-section from 0.25 $Å^2$ to 0.56 $Å^2$, the Max-Vel value increases from 0.01 Å/ps to 0.014 Å/ps. The process described in this part demonstrates that by increasing the cross-sectional area, the power of HT in the sample can be increased, which can be expressed and proven by performing calculations related to the HF and TC of the simulated base fluid.

In this part's final stage, the samples' HF and TC are calculated and reported according to the cross-sectional area of the platinum MC. Fig. 15 represents the changes in the HF of the EG fluid inside the platinum MC according to the cross-section of the MC. According to the results obtained from the graph, the sufficient time for establishing thermal equilibrium in the simulated sample is 10 ns. based on these graphs, it can be said that 10 ns is enough time to establish thermal equilibrium in the simulated sample. Therefore after this time, the

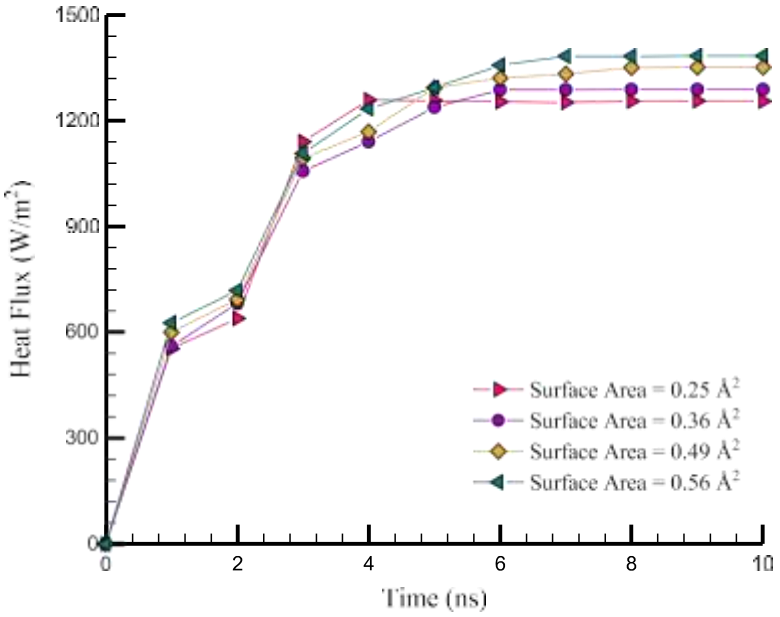

Fig. 15. Changes in the HF according to the cross-sectional area of the MC.

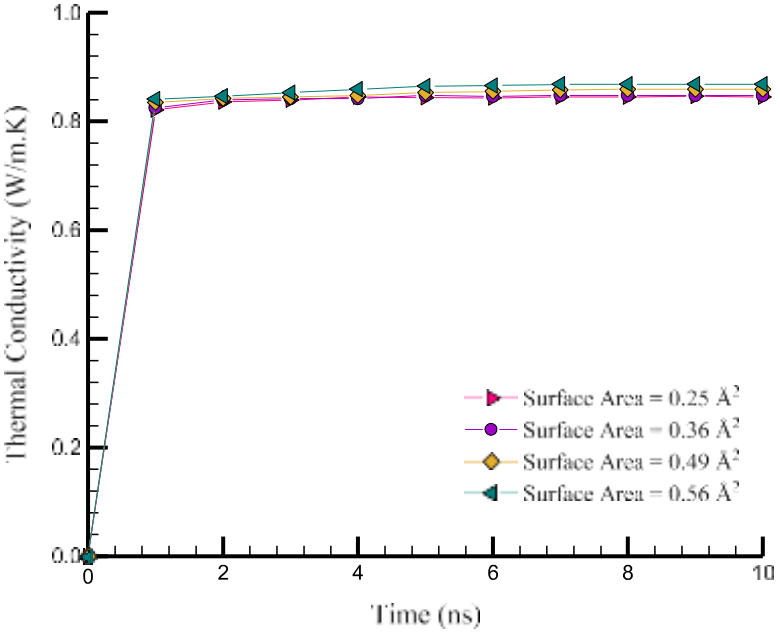

Fig. 16. Changes in the TC according to the cross-sectional area of the MC.

Table 3

Numerical results of simulated structure in terms of MC cross-section.

MC cross section ($Å^2$)	Max-Dens (atom/$Å^3$)	Max-Vel (Å/ps)	Max-Temp (K)	HF (W/m^2)	TC (W/m.K)
0.25	0.025	0.010	514.353	1253	0.845
0.36	0.022	0.012	589.331	1286	0.848
0.49	0.018	0.013	618.001	1349	0.859
0.56	0.016	0.014	691.639	1381	0.868

amount of HF in the sample with a cross-sectional area of 0.25, 0.36, 0.49, and 0.56 $Å^2$ are equal to 1253, 1286, 1349, and 1381 W/m^2, respectively. As a result, with the increase of the cross-section of the MC, the amount of HF inside it increases. This increase is defined as the result of an increase in the atomic mobility and the oscillating amplitude of the fluid.

Considering that there is a direct relationship between the transferred HF and the conductivity coefficient of atomic samples, the increase of the HF will correspond to the TC. Fig. 16 illustrates the changes in the TC of the EG fluid inside the platinum MC according to the cross-section of the MC. The value of the TC in the sample has an increasing trend with the increase of the cross-section of the channel. The numerical results represent an increase in the TC from 0.845 to 0.868 $W/m.K$ W/m.K due to the increase in the cross-sectional area of the MC from 0.25 to 0.56 $Å^2$ (see Table 3).

The Numerical results of the platinum MC and EG fluid sample in terms of MC cross-sectional area at the Temp of 300 K and after 10 ns are presented in Table 3.

Generally, the MCs can be used in the field of pumps, microchip cooling, air conditioning, etc. Therefore, it is possible to improve the TB

inside these MCs by adjusting the wall Temp or channel dimensions.

3. Conclusion

The current research investigated EG fluid's atomic and TB inside the platinum MC. For this purpose, computer simulations were used, and the MD simulation method was used to be more precise. From a technical point of view, the simulations carried out in this research included two main stages balancing the atomic samples and establishing the atomic and thermal transformation. The results obtained in the balancing stage indicated the thermodynamic balance of the structure in the defined initial conditions (Temp of 300 K). The equilibrium process was investigated in 10 ns. In the second step, the samples were studied again for 10 ns, and their atomic and TB was checked using the Green Kobo method. The overall results obtained in this part of the research were as follows:

- Balance in atomic samples due to the convergence of physical quantities, including Temp and KE, is 300 K, 17.35 eV. On the other hand, these convergences indicate that the duration of 10 ns is sufficient to balance the structures.
- Increasing the Temp difference between the wall from 0 to 50 K has increased the Max-Temp and Max-Vel from 514.35 to 640.94 K (about 25%) and from 0.01 to 0.024 Å/ps (more than twice), respectively.
- By increasing the Temp difference between the wall from 10 to 50 K, the amount of HF and TC increased from 1356 W/m^2 and 0.849 $W/m.K$ to 1459 W/m^2 (about 8%) and 0.903 $W/m.K$ (about 7%). As a result, the HT in industrial cases is expected to increase by increasing the Temp difference in the designed sample
- By increasing the cross-sectional area from 0.25 $Å^2$ to 0.56 $Å^2$, the Max-Temp and Max-Vel value increased from 514.353 to 691.639 (about 34%) K and from 0.01 to 0.014 Å/ps (about 40%). So, by increasing the cross-sectional area, the power of HT in the sample can be increased.
- Increasing the cross-sectional area from 0.25 $Å^2$ to 0.56 $Å^2$ has increased the values of HF and TC from 1253 W/m^2 and 0.845 $W/m.K$ to 1381 W/m^2 (about 10%) and 0.868 $W/m.K$ (about 3%). This increase is defined as the result of an increase in the atomic mobility and the oscillating amplitude of the fluid.

Declaration of Competing Interest

The authors declare that they have no known competing financial interests or personal relationships that could have appeared to influence the work reported in this paper.

Data availability

Data will be made available on request.

Acknowledgement

This work is supported by the Science Foundation of Donghai Laboratory (No. DH-2022KF0302). The research leading to these results has received funding from the Norwegian Financial Mechanism 2014-2021 under Project Contract No 2020/37/K/ST8/02748.

References

[1] Rebrov EV, Schouten JC, De Croon MH. Single-phase fluid flow distribution and heat transfer in microstructured reactors. Chem Eng Sci 2011;66(7):1374–93.
[2] Choi SU, Eastman JA. Enhancing thermal conductivity of fluids with nanoparticles 1995.
[3] Saffarian MR, Moravej M, Doranehgard MH. Heat transfer enhancement in a flat plate solar collector with different flow path shapes using nanofluid. Renew Energy 2020;146:2316–29.
[4] Sarbu I, Dorca A. Review on heat transfer analysis in thermal energy storage using latent heat storage systems and phase change materials. Int J Energy Res 2019;43(1):29–64.
[5] Xu HJ, Xing ZB, Wang F, Cheng Z. Review on heat conduction, heat convection, thermal radiation and phase change heat transfer of nanofluids in porous media: fundamentals and applications. Chem Eng Sci 2019;195:462–83.
[6] Zhang J, Zhu X, Mondejar ME, Haglind F. A review of heat transfer enhancement techniques in plate heat exchangers. Renew Sust Energ Rev 2019;101:305–28.
[7] Yue H, Zhao Y, Ma X, Gong J. Ethylene glycol: properties, synthesis, and applications. Chem Soc Rev 2012;41(11):4218–44.
[8] Harris JM. Poly (ethylene glycol) chemistry: biotechnical and biomedical applications. Springer Science & Business Media; 1992.
[9] Zalipsky S, Harris JM. Introduction to chemistry and biological applications of poly (ethylene glycol). ACS Publications; 1997.
[10] Ibrahim RK, Hayyan M, AlSaadi MA, Ibrahim S, Hayyan A, Hashim MA. Physical properties of ethylene glycol-based deep eutectic solvents. J Mol Liq 2019;276:794–800.
[11] Guo J, Xu M, Cai J, Huai X. Viscous dissipation effect on entropy generation in curved square microchannels. Energy 2011;36(8):5416–23.
[12] Bagheri S, Rastad S, Oloomi SAA, Negahi AH, Ashtian Malayer M. Numerical investigation of heat transfer in serpentine microchannel with Al2O3/water and CuO/water nanofluids. Iran J Mech Eng 2019;21(2):56–74.
[13] Wu H, Torkian P, Zarei A, Moradi I, Karimipour A, Afrand M. Hydrodynamic and thermal flow in nanochannel to study effects of roughness by estimation the atoms positions via MD method. Int J Numer Methods Heat Fluid Flow 2020;30(1):452–67.
[14] Kalteh M, Abbassi A, Saffar-Avval M, Harting J. Eulerian–Eulerian two-phase numerical simulation of nanofluid laminar forced convection in a microchannel. Int J Heat Fluid Flow 2011;32(1):107–16.
[15] S. Rostami, H. Ahmadi-Danesh-Ashtiani, D. Toghraie, R. Fazaeli, A statistical method for simulation of boiling flow inside a Platinum microchannel. Phys A: Stat Mech Appl 2020;548,123879.
[16] Hu X, Derakhshanfard AH, Khalid I, Jalil AT, Opulencia MJC, Dehkordi RB, Toghraie D, Hekmatifar M, Sabetvand R. The microchannel type effects on water-Fe_3O_4 nanofluid atomic behavior: molecular dynamics approach. J Taiwan Inst Chem Eng 2022;135:104396.
[17] Shang Y, Dehkordi RB, Chupradit S, Toghraie D, Sevbitov A, Hekmatifar M, Suksatan W, Sabetvand R. The computational study of microchannel thickness effects on H_2O/CuO nanofluid flow with molecular dynamics simulations. J Mol Liq 2022;345:118240.
[18] Chen CH, Ding CY. Study on the thermal behavior and cooling performance of a nanofluid-cooled microchannel heat sink. Int J Therm Sci 2011;50(3):378–84.
[19] Marx D, Hutter J. Ab initio molecular dynamics: basic theory and advanced methods. Cambridge University Press; 2009.
[20] Marx D, Hutter J. Ab initio molecular dynamics: Theory and implementation. Modern methods Algorithms Quantum Chem 2000;1(301–449):141.
[21] Ercolessi F. A molecular dynamics primer", Spring college in computational physics. ICTP, Trieste 1997;19.
[22] Rapaport DC, Rapaport DCR. The art of molecular dynamics simulation. Cambridge university press; 2004.
[23] Swope WC, Andersen HC, Berens PH, Wilson KR. A computer simulation method for the calculation of equilibrium constants for the formation of physical clusters of molecules: application to small water clusters. J Chem Phys 1982;76(1):637–49.
[24] Hairer E, Lubich C, Wanner G. Geometric numerical integration illustrated by the Störmer–Verlet method. Acta Numer 2003;12:399–450.
[25] Green MS. Markoff random processes and the statistical mechanics of time-dependent phenomena. II. Irreversible processes in fluids. J Chem Phys 1954;22(3):398–413.
[26] Frenkel D, Smit B. Molecular simulation: from algorithms to applications. New York: Academic Press; 2000.
[27] Berendsen H, Grigera J, Straatsma T. The missing term in effective pair potentials. J Phys Chem 1987;91(24):6269–71.
[28] Rappé AK, Casewit CJ, Colwell K, Goddard III WA, Skiff WM. UFF, a full periodic table force field for molecular mechanics and molecular dynamics simulations. J Am Chem Soc 1992;114(25):10024–35.
[29] Tee LS, Gotoh S, Stewart WE. Molecular parameters for normal fluids. Lennard-Jones 12-6 Potential. Ind Eng Chem Fundam 1966;5(3):356–63.
[30] Daw MS, Baskes MI. Embedded-atom method: derivation and application to impurities, surfaces, and other defects in metals. Phys Rev B 1984;29(12):6443.
[31] Asgari A, Nguyen Q, Karimipour A, Bach QV, Hekmatifar M, Sabetvand R. Investigation of additives nanoparticles and sphere barriers effects on the fluid flow inside a nanochannel impressed by an extrinsic electric field: a molecular dynamics simulation. J Mol Liq 2020;318:114023.
[32] Mosavi A, Hekmatifar M, a. Alizadeh A, Toghraie D, Sabetvand R, Karimipour A. The molecular dynamics simulation of thermal manner of Ar/Cu nanofluid flow: the effects of spherical barriers size. J Mol Liq 2020;319:114183.